



SAG/RBX2 E3 Ubiquitin Ligase Differentially Regulates Inflammatory Responses of Myeloid Cell Subsets

Xiufang Xiong^{1,2†}, Nathan D. Mathewson^{3,4,5†}, Hua Li², Mingjia Tan², Hideaki Fujiwara³, Haomin Li⁶, Pavan Reddy^{3*} and Yi Sun^{1,2*}

¹ Institute of Translational Medicine, and Cancer Institute of the Second Affiliated Hospital, Zhejiang University School of Medicine, Hangzhou, China, ² Department of Radiation Oncology, University of Michigan, Ann Arbor, MI, United States, ³ Division of Hematology and Oncology, Department of Internal Medicine, University of Michigan Comprehensive Cancer Center, Ann Arbor, MI, United States, ⁴ Graduate Program in Immunology, University of Michigan Medical School, Ann Arbor, MI, United States, ⁵ Department of Cancer Immunology and Virology, Department of Microbiology and Immunobiology, Department of Neurology, Dana-Farber Cancer Institute, Harvard Medical School, and Brigham and Women's Hospital, Boston, MA, United States, ⁶ Children's Hospital, Zhejiang University School of Medicine, Hangzhou, China

OPEN ACCESS

Edited by:

Uday Kishore,
Brunel University London,
United Kingdom

Reviewed by:

Jaya Talreja,
Wayne State University School of
Medicine, United States
Trinath Jamma,
Birla Institute of Technology and
Science, India

*Correspondence:

Yi Sun
sunyj@umich.edu;
yisun@zju.edu.cn
Pavan Reddy
reddypr@med.umich.edu

[†]These authors have contributed
equally to this work

Specialty section:

This article was submitted to
Molecular Innate Immunity,
a section of the journal
Frontiers in Immunology

Received: 22 September 2018

Accepted: 23 November 2018

Published: 06 December 2018

Citation:

Xiong X, Mathewson ND, Li H, Tan M,
Fujiwara H, Li H, Reddy P and Sun Y
(2018) SAG/RBX2 E3 Ubiquitin Ligase
Differentially Regulates Inflammatory
Responses of Myeloid Cell Subsets.
Front. Immunol. 9:2882.
doi: 10.3389/fimmu.2018.02882

Macrophages form an important component of the innate immune system and serve as first responders against invading pathogens. While pathways critical for initiation of inflammatory responses between macrophages and other LysM⁺ myeloid cells are largely similar, it remains unknown whether a specific pathway has differential effects on inflammatory responses mediated between these cells. Recent studies demonstrated that depletion of SAG (Sensitive to Apoptosis Gene), an E3 ubiquitin ligase, blocked inflammatory responses generated by macrophages and dendritic cells in response to LPS in cell culture settings. However, the *in vivo* role of Sag on modulation of macrophages and neutrophil is not known. Here we generated LysM-Cre/Sag^{fl/fl} mice with selective Sag deletion in myeloid lineage, and found that in contrast to *in vitro* observations, LysM-Cre/Sag^{fl/fl} mice showed increased serum levels of proinflammatory cytokines and enhanced mortality in response to LPS. Interestingly, while Sag^{-/-} macrophages released less proinflammatory cytokines, Sag^{-/-} neutrophils released more. Mechanistically, expression of a list of genes response to LPS was significantly altered in bone marrow cells from LysM-Cre⁺/Sag^{fl/fl} mice after LPS challenge. Specifically, induction by LPS of myeloperoxidase (Mpo), a key neutrophil enzyme, and Elane, neutrophil expressed elastase, was significantly decreased upon Sag depletion. Collectively, our study revealed that Sag plays a differential role in the activation of macrophages and neutrophils.

Keywords: inflammatory response, macrophage, neutrophil, SAG ubiquitin ligase, LPS

INTRODUCTION

The innate immune system consists of several cell types and is the first line of defense in the host, functioning as a barrier to infection from invading organisms (1). Macrophages and neutrophils, two cell types of the innate immune system, derive from the myeloid progenitor lineage that are critical for the initiation of inflammation in the context of antimicrobial immunity (2). Innate immune cells recognize and bind to pathogen associated molecular patterns (PAMPs) of pathogens

via pattern recognition receptors (PRRs). Toll-like receptors (TLRs), a type of PRR, regardless of the innate immune cells that express them, utilize similar signal pathways that lead to the activation of the nuclear factor-kappa B (NF- κ B) pathway (3) and initiates the release of proinflammatory cytokines (4, 5). These mutual and complementary features of innate immune cells likely favor their interaction and cooperation in generating complimentary innate immune responses (2). However, whether there are differences in the mechanisms through which specific innate immune cells are activated in response to infection remains unknown. In this context, specifically, whether the critical LysM-enzyme expressing innate immune cells—namely macrophages and neutrophils—utilize the same pathway to produce differential inflammatory responses is not known.

SAG, also known as RING box protein 2 (RBX2), Regulator of Cullins 2 (ROC2), or RING Finger Protein 7 (RNF7)—was originally cloned by differential display in our laboratory (6, 7). As a member of the Cullin-RING ligase (CRL) E3 ubiquitin ligase complex, SAG binds to ubiquitin-loaded E2 and catalyzes the ubiquitin transfer from the E2 molecule to a substrate for subsequent degradation by the proteasome. By promoting the degradation of a variety of substrates through its ligase activity, SAG regulates diverse signaling pathways and biological processes, including cell apoptosis, embryonic development, vasculogenesis, angiogenesis, and tumorigenesis (8). SAG was previously reported to maintain macrophage survival and to regulate the levels of inflammatory cytokines in response to infection by ubiquitinating the pro-apoptotic proteins Bax and SARM (9, 10). Further, inhibitor of κ B (I κ B α), a classical inhibitor of NF- κ B activation, is a direct substrate of the SAG-CRL1 ^{β -TrCP} E3 ubiquitin ligase (11). In addition, SAG is also one of several E3 ligases for neddylation, which is required for CRL activation by cullin neddylation (12). Accumulating studies have shown that neddylation pathway regulates Lipopolysaccharide (LPS)-induced proinflammatory cytokine production in macrophages by blocking CRL-mediated I κ B α degradation to retain NF- κ B in the cytoplasm (10, 13).

It is well-known that the activation and translocation of NF- κ B to the nucleus is responsible for the transcription of the proinflammatory cytokines tumor necrosis factor- α (TNF α) and interleukin-6 (IL-6) (14, 15). The accumulation of I κ B upon SAG disruption leads to the inhibition of NF- κ B activation and thus decreases inflammatory responses by dendritic cells (DCs) *in vitro* (16). Thus, inhibition of SAG may regulate the innate immune response of macrophages in a similar manner as in DCs (16).

LysM⁺ cells (i.e., macrophages and neutrophils) are the keys to the *in vivo* inflammatory response. In light of the regulation of NF- κ B by SAG, we tested the hypothesis that SAG deficient LysM⁺ cells would release less proinflammatory cytokines in response to LPS and mitigate LPS-induced mortality. Surprisingly, we found that loss of SAG protein in these cells resulted in a net increase in proinflammatory cytokines and furthermore increased LPS-induced mortality. Mechanistic studies showed that disruption of SAG in macrophages, is consistent with previous reports (9), reduced the release of inflammatory cytokines by preventing

the degradation of I κ B α and thus inhibited subsequent NF- κ B activation. By contrast, SAG deficiency in neutrophils up-regulated the release of inflammatory cytokines with no change on nuclear translocation of NF- κ B after LPS stimulation. Furthermore, microarray analysis revealed that induction of myeloperoxidase (Mpo), a key neutrophil enzyme (17), and Elane, neutrophil expressed elastase (18), was significantly decreased in bone marrow cells from LysM-Cre⁺/SAG^{fl/fl} mice in response to LPS, which likely contributed to the net increase in systemic levels of proinflammatory cytokines and increased LPS-induced mortality in response to LPS *in vivo*. Taken together, these findings suggest that the same molecule—namely SAG—plays a differential role in the activation of macrophages and neutrophils.

MATERIALS AND METHODS

Reagents

RPMI, penicillin and streptomycin, and sodium pyruvate were purchased from Gibco (Grand Island, NY); FCS from GemCell (Sacramento, CA); 2-ME from Sigma (St. Louis, MO); murine GM-CSF from Peprotech (Rocky Hill, NJ). All antibodies (Abs) used for FACS were purchased from eBioscience (San Diego, CA). DMSO and lipopolysaccharide (LPS) was purchased from Sigma (St. Louis, MO).

Mouse Studies

The SAG^{fl/fl} mice were generated as previously described (19, 20). The LysM-cre mice were purchased from the Jackson Laboratory (Stock number: 004781). Male and female mice used were between 8 and 12 weeks of age. All procedures were approved by the University of Michigan Committee on Use and Care of Animals. Animal care was provided in accordance with the principles and procedures outlined in the National Research Council Guide for the Care and Use of Laboratory Animals.

LPS Administration

Mice at 8 weeks old were subjected to i.p. injection of *Escherichia coli* LPS (0111:B4, Sigma, L4391) at 25 mg/kg body weight and were monitored for survival. For short-term studies, mice were sacrificed 18 h post LPS i.p. injection, followed by blood collection with cardiac puncture. Peritoneal cavity was then washed with PBS and spleens were collected.

Macrophage Preparation

For BMDM preparation, bone marrow cells were flushed from the femurs and tibiae of mice and cultured in complete RPMI in the presence of 20% medium conditioned by L929 mouse fibroblasts, as described (21). On day 7, BMDMs were split and used as indicated. To isolate thioglycollate-elicited macrophages, mice were i.p. injected with 1.5 ml of 5% thioglycollate and peritoneal macrophages were flushed out 3 days post-injection.

Cytokine Detection

Isolated peritoneal macrophages (85% pure CD11b⁺/F4.80⁺ macrophages) were seeded on six-well plates at 3×10^6 cells/well. Unstimulated and LPS-stimulated cells were cultured

for indicated period. Supernatants were subsequently collected and stored at -20°C until analysis. TNF α and IL-6 ELISA kits were purchased from R&D Systems and performed as per the manufacturers' instructions and read at 450 nm by a SpectraMax microplate reader (Molecular Devices, Sunnyvale, CA).

Flow Cytometry

To examine macrophages by flow cytometry, cells were analyzed from either the spleen or peritoneal cavity and gated on CD11b⁺ and F4/80⁺ double positive cells (**Supplemental Figure 2**). Briefly, spleens were isolated and disrupted to a single cell suspension between two frosted slides in RPMI supplemented with 10% FCS, 4 mM L-glutamine, 10 U/ml penicillin, 100 $\mu\text{g}/\text{ml}$ streptomycin, 0.5 mM 2-ME. Cells were then washed and resuspended in FACS buffer (PBS supplemented with 2% FBS) and stained with indicated flow cytometry antibodies. For analysis of peritoneal macrophages and neutrophils, euthanized animals were injected with 5 ml ice cold PBS supplemented with 3% FBS into the peritoneum following the removal of the outer layer of skin exposing the peritoneal lining. The abdomen was next massaged and the fluid was withdrawn using a 25 G needle, bevel up. The cells were washed, resuspended in FACS buffer, and stained with indicated flow cytometry antibodies.

To analyze macrophage surface phenotype, macrophages were incubated in the presence or absence of LPS. Cells were then harvested, stained, and gated on CD11b-conjugated FITC (Clone: M1/70) and F4.80-conjugated APC with the following per triplicate group: Annexin V (BD Biosciences), CD80 (Clone: 16-10A1), CD86 (Clone: GL-1), CD40 (Clone: 3/23), MHCII-I-Ab (Clone: AF6-120.1), PD-L1 (Clone: MIH5), PD-L2 (Clone: TY25). The total numbers of cells expressing the indicated phenotypes were determined by factoring the total cell counts (**Supplemental Figure 1**) with the percent expression of gated markers, taking into account the parent population gates.

Analysis of neutrophils from the spleen and peritoneum (cell preparation described above) were gated on Gr-1 conjugated FITC (RB6-8C5) and CD11b-conjugated PerCP/Cy5.5 (M1/70) (**Supplemental Figure 2**).

Cytokine measurement by flow cytometry was analyzed by gating on macrophages (CD11b⁺ and F4/80⁺ double positive cells) or neutrophils (Gr-1⁺ and CD11b⁺ double positive cells) following the incubation of splenocytes or peritoneal cells with golgi block for 6 h. Cells were stained with TNF α -conjugated APC (MP6-XT22) and IL-6 (MP5-20F3). Total number of cells producing indicated cytokine was calculated by factoring the total number of cells indicated in **Table 3** by the percent expression of gated markers, taking into account the parent population gates.

Propidium iodide was obtained from BD bioscience and used according to the manufacturers' instructions. All flow cytometry Abs were purchased from eBiosciences. Stained cells were then analyzed with an Accuri C6 Flow Cytometer (BD Biosciences).

ATPlite Assay

BMDM cells were seeded into 96-well plates with 5,000 cells per well in triplicate and treated with various concentrations of LPS for 3 days followed by ATPlite assay using an ATPlite kit (Perkin Elmer) according to the manufacturer's instructions.

Western Blot Analysis

BMDM cells stimulated with LPS for different time periods were harvested, lysed and subjected to Western blotting, using various antibodies as follows: Sag monoclonal mouse antibody was raised against the RING domain (AA44-113) (22), Roc1 polyclonal rabbit antibody (23), $\text{pho-I}\kappa\text{B}\alpha$ (Cell Signaling), $\text{I}\kappa\text{B}\alpha$ (Santa Cruz), p65 (Santa Cruz), Parp (Cell Signaling), Procaspase-3 (Santa Cruz), and actin (Sigma), as a loading control.

Nuclear-Cytoplasmic Fractionation

Cells were treated with or without LPS (100 ng/ml) as control for 1 h, then cells were washed with cold PBS and collected by scraping followed by the addition of lysis buffer A [10 mM HEPES, pH 8.0, 10 mM NaCl, 1.5 mM MgCl_2 , 1 mM DTT, 0.1% NP-40 and a protease inhibitor cocktail (Roche)]. Lysis was completed on ice for 10 min. Supernatants containing the cytoplasmic fractions were collected after centrifugation (400 g, 4°C , 5 min). The pellets were washed three times in lysis buffer A and then lysed in buffer B (20 mM HEPES, pH 8.0, 20% glycerol, 500 mM NaCl, 1.5 mM MgCl_2 , 0.2 mM EDTA, pH 8.0, 1 mM DTT, and a protease inhibitor cocktail) for 30 min on ice, then centrifuged at 15,000 g, 4°C for 15 min. The supernatants containing nuclear lysates were collected.

Neutrophil Isolation From Blood

Blood was carefully layered over neutrophil separation media, followed by centrifugation at 500 g for 35 min at room temperature. The layer of neutrophils and all of the isolation media beneath the neutrophils were carefully collected and then diluted to 10 ml with HBSS without $\text{Ca}^{2+}/\text{Mg}^{2+}$. Cells were suspended and then collected by centrifugation at 350 g for 10 min. The residual red blood cells were lysed by Red Cell Lysis Buffer (Roche), followed by centrifugation at 250 g for 5 min.

Microarray Analysis

Mice were i.p. injected with PBS or LPS (25 mg/kg body weight). The bone marrow cells were flushed out 6 h post injection, followed by RNA extraction and subsequent microarray analysis using Mouse Gene ST 2.1 Strip (Affymetrix). The expression values for each gene was calculated using a robust multi-array average (24). Probeset that had a 2-fold or greater change with the added constraint that the expression value of one of the two samples was 2^3 or greater were selected. The expression of genes was compared in WT or KO bone marrow in response to LPS stimulation. Gene list that only changed in KO were enhanced using GO enrichment analysis of ConsensusPathDB (25). The expression heatmap of selected gene list were generated under R (version 3.4.0).

Gene Expression

Total RNA was isolated from cells with Trizol reagent (Invitrogen). Complementary DNA was made from RNA with Superscript III (Invitrogen) and subjected to reverse transcription PCR or quantitative real-time PCR (qRT-PCR)

with a 7,500 Real Time PCR system (Applied Biosystems). The cycling program for qRT-PCR was set as follows: 50°C 2 min, 95°C 10 min for the PCR initial activation and 45 cycles of denaturation at 95°C for 15 s, annealing and extension at 60°C for 1 min. The sequences of Sag, TNF α , IL-6, Mpo, Elane, LitaF, and GAPDH are as follows: Sag-Fwd: 5'- CGC TGA GCC ACC GTA CCT - 3', Sag-Rev: 5'- TTA CAC TCT CCC CAG ACC

ACA A - 3'; TNF α -Fwd: 5'- CCC CAA AGG GAT GAG AAG TT - 3', TNF α -Rev: 5'- CTT GGT GGT TTG CTA CGA CG - 3'; IL6-Fwd: 5'- TCA TAT CTT CAA CCA AGA GGT AAA A - 3', IL6-Rev: 5'- CGC ACT AGG TTT GCC GAG TA - 3'; Mpo-Fwd: 5'- ATC ACG GCC TCC CAG GAT AC - 3', Mpo-Rev: 5'- GTT GTT GGG CGT GCC ATA TT - 3', Elane-Fwd: 5'- CAG GCA TCT GCT TCG GGG A - 3', Elane-Rev: 5'- GGG ATG GGT AAG

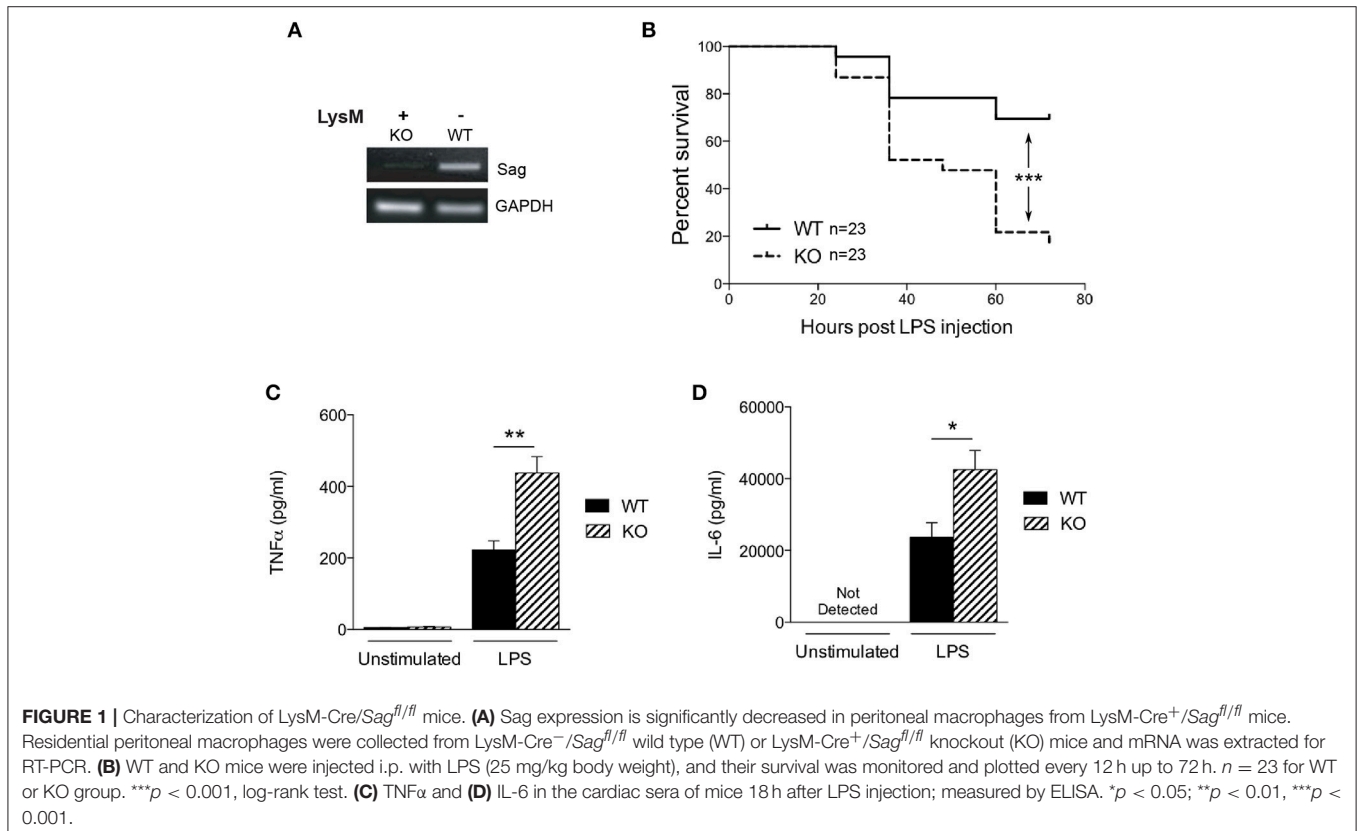


TABLE 1 | Mouse CBC.

Parameter	Unit	4 Weeks			12 Weeks		
		WT (LysM ⁻)	KO (LysM ⁺)	<i>P</i> value	WT (LysM ⁻)	KO (LysM ⁺)	<i>P</i> value
WBC#	K/ μ L	3.72 \pm 0.07	4.08 \pm 1.52	0.65	7.67 \pm 1.24	7.64 \pm 3.27	0.88
NE#	K/ μ L	0.54 \pm 0.13	0.42 \pm 0.07	0.11	1.98 \pm 1.08	1.96 \pm 1.00	0.52
LY#	K/ μ L	2.99 \pm 0.17	3.38 \pm 1.34	0.59	5.01 \pm 0.89	5.08 \pm 1.83	0.67
MO#	K/ μ L	0.16 \pm 0.03	0.26 \pm 0.14	0.24	0.38 \pm 0.09	0.49 \pm 0.33	0.47
EO#	K/ μ L	0.02 \pm 0.03	0.02 \pm 0.02	0.99	0.23 \pm 0.37	0.08 \pm 0.11	0.15
BA#	K/ μ L	0.00 \pm 0.01	0.00 \pm 0.00	0.88	0.07 \pm 0.05	0.04 \pm 0.06	0.54
RBC	M/ μ L	5.70 \pm 0.26	6.66 \pm 2.12	0.40	9.41 \pm 2.10	10.55 \pm 0.88	0.41
HB	g/dL	8.38 \pm 0.58	9.46 \pm 2.73	0.47	12.97 \pm 2.64	14.7 \pm 0.42	0.31
HCT	%	29.68 \pm 1.63	33.86 \pm 10.03	0.44	48.43 \pm 11.03	52.75 \pm 2.52	0.64
PLT	K/ μ L	469.8 \pm 51.9	543.4 \pm 150.4	0.39	689.7 \pm 126.3	725.5 \pm 165.4	0.82
MPV	fL	3.82 \pm 0.26	4.18 \pm 0.60	0.31	4.23 \pm 1.22	4.12 \pm 0.33	0.31

WBC, absolute number of white blood cells; NE, absolute number of neutrophils; LY, absolute number of lymphocytes; MO, absolute number of monocytes; EO, absolute number of eosinophils; BA, absolute number of basophils; RBC, absolute number of red blood cells; HB, hemoglobin; HCT, hematocrit; PLT, absolute number of platelets; MPV, mean platelet volume. Shown are mean \pm SD. *n* = 4 for WT, *n* = 5 for KO.

TABLE 2 | Mouse naïve phenotype.

	Marker	WT (LyzM ⁻)	KO (LyzM ⁺)	P value
Spleen	Total count	4.18e7 ± 7.10e6	4.47e6 ± 1.25e6	0.60
	CD11b/F4.80	1.81e6 ± 1.96e5	1.95e6 ± 1.37e5	0.55
	MHCII	1.53e6 ± 1.53e5	1.65e6 ± 1.11e5	0.66
	CD80	1.29e6 ± 2.01e5	1.41e6 ± 1.29e5	0.50
	CD86	1.07e6 ± 1.70e5	1.21e6 ± 8.09e4	0.88
	CD40	1.89e5 ± 6.99e4	1.77e5 ± 2.67e4	0.67
	PDL1	1.22e6 ± 1.56e5	1.31e6 ± 1.09e5	0.90
	PDL2	3.08e5 ± 9.94e4	3.23e5 ± 1.10e4	0.60
Bone marrow	Total count	2.64e7 ± 2.01e6	2.32e7 ± 2.95e6	0.89
	CD11b/F4.80	7.60e6 ± 1.19e6	7.80e6 ± 4.70e5	0.48
	MHCII	2.28e6 ± 4.01e5	1.93e6 ± 2.19e5	0.87
	CD80	1.21e6 ± 2.43e5	1.25e6 ± 1.28e5	0.42
	CD86	1.14e6 ± 2.84e5	1.40e6 ± 3.53e4	0.20
	CD40	1.80e5 ± 1.99e4	2.56e5 ± 4.59e4	0.62
	PDL1	6.41e5 ± 1.34e5	7.31e5 ± 9.92e4	0.11
	PDL2	1.73e5 ± 3.61e3	3.21e5 ± 7.12e3	0.89
Peripheral lymph nodes	Total count	6.29e6 ± 1.69e6	8.39e6 ± 5.87e5	0.81
	CD11b/F4.80	2.67e5 ± 5.14e4	2.81e5 ± 1.82e4	0.79
	MHCII	2.60e5 ± 5.04e4	2.75e5 ± 1.93e4	0.59
	CD80	1.25e5 ± 2.58e4	1.42e5 ± 1.21e4	0.79
	CD86	2.07e5 ± 2.86e4	2.20e5 ± 2.28e4	0.51
	CD40	3.43e4 ± 9.63e3	2.64e4 ± 5.26e3	0.67
	PDL1	2.01e5 ± 3.72e4	2.19e5 ± 1.29e4	0.60
	PDL2	7.06e4 ± 1.89e4	5.81e4 ± 1.10e4	0.81

Shown are mean ± SD. *n* = 8 for WT, *n* = 8 for KO.

AAG GTG GTC A - 3', LitaF-Fwd: 5' - CAG TCT GTG TCT GCT GGG ATG C - 3', LitaF-Rev: 5' - ACT ACC TCT GCA GTG GCG GG - 3', GAPDH-Fwd: 5' - GCC GCC TGG AGA AAC CTG CC - 3', GAPDH-Rev: 5' - GGT GGA AGA GTG GGA GTT GC - 3'.

Statistical Analysis

Bars and error bars represent the means and standard errors of the mean, respectively. The two-tailed Student *t*-test was used for the comparison of parameters between groups. Survival analysis was performed by Kaplan-Meier analysis. Statistical significance was determined as **p* < 0.05; ***p* < 0.01; ****p* < 0.001.

RESULTS

Characterization of LysM-Cre/Sag^{fl/fl} Mice

To determine the role of SAG in the innate inflammatory response—specifically macrophages—we crossed *Sag*^{fl/fl} mice with LysM-Cre transgenic mice, which express Cre recombinase in myeloid cells (26). Inactivation of *Sag* was verified in macrophages of the peritoneal cavity by RT-PCR analysis (Figure 1A). The mRNA levels of *Sag* were significantly decreased in resident peritoneal macrophages from LysM-Cre⁺/*Sag*^{fl/fl} (KO) mice compared to LysM-Cre⁻/*Sag*^{fl/fl} (WT) mice. To determine whether hematopoietic deficiency of *Sag* in LysM⁺ cells affects their development and/or other cells, we

performed serial complete blood count (CBC) analysis of mice at 4 and 12 weeks of age. *Sag*-deficiency in the myeloid lineage had no significant effect on the total cell numbers of white blood cells, neutrophils, lymphocytes, monocytes, eosinophils, basophils, red blood cells, and platelets in the peripheral blood (Table 1).

Next, we determined whether *Sag* deficiency affected the phenotype of macrophages by performing immunophenotypical analysis of macrophages isolated from the spleen, bone marrow, and peripheral lymph nodes. No significant differences were observed between WT and KO animals in either the absolute numbers or percentages of macrophages (CD11b⁺ and F4/80⁺) or the expression of co-stimulatory molecules (MHCII, CD80, CD86, CD40, PD-L1, PD-L2 (Table 2 and Supplemental Figure 1). These data indicate that targeted deletion of *Sag* in the myeloid lineage does not result in significant altered development, total numbers, or phenotype of these cells.

The *in vivo* Responses of Sag-Deficiency in Myeloid Lineage to LPS

Previous studies have shown that SAG knockdown in macrophages results in decreased release of inflammatory cytokines upon LPS stimulation (9, 10). Therefore, we next

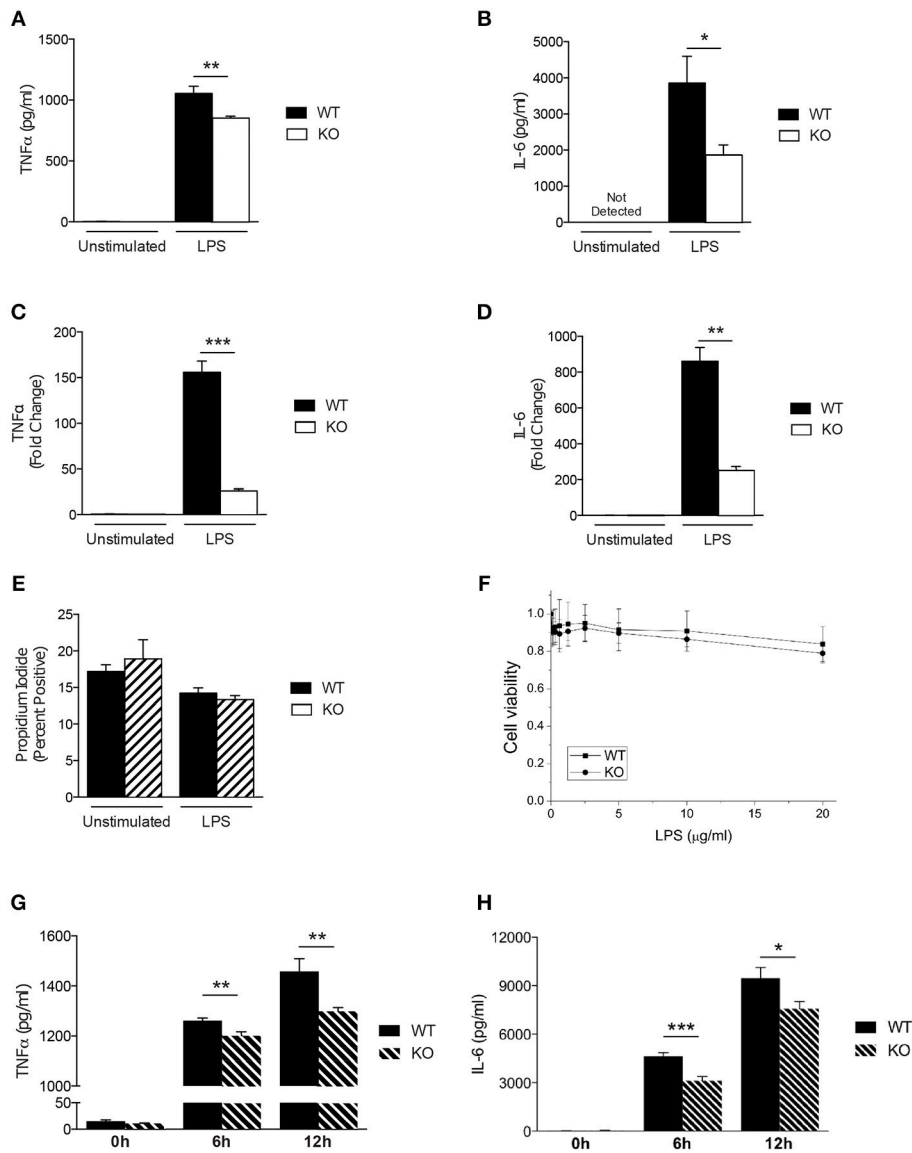


FIGURE 2 | Characterization of Sag-deficient macrophages *in vitro*. (A–D) Reduced production of proinflammatory cytokines in thioglycollate-elicited peritoneal macrophages from LysM-cre/Sag^{fl/fl} mice. Cells culture supernatants were analyzed from either unstimulated or stimulated macrophages with 100 ng/ml LPS for 24 h. TNFα and IL-6 protein concentrations were measured by (A,B) ELISA and (C,D) mRNA transcripts in cells by qPCR. (E,F) Sag deficiency has no effect on the (E) apoptosis (Annexin V/PI) of peritoneal macrophages or (F) viability of BMDMs in response to LPS. The peritoneal macrophages derived from LysM-cre/Sag^{fl/fl} mice were treated with 100 ng/ml LPS for 72 h (E). The viability of BMDMs treated with various concentrations of LPS for 72 h in triplicates were normalized to untreated cells and shown as mean ± SEM (*n* = 2) (F). (G,H) Reduced production of proinflammatory cytokines in BMDMs derived from LysM-cre/Sag^{fl/fl} mice. BMDMs were stimulated with 100 ng/ml LPS for 6 and 12 h. (G) TNFα and (H) IL-6 release were measured in cell culture supernatants by ELISA. **p* < 0.05; ***p* < 0.01; ****p* < 0.001.

tested the hypothesis whether *in vivo* LPS stimulation would result in decreased proinflammatory cytokines and decreased mortality in KO animals. We injected intraperitoneally (i.p) WT and KO littermate mice with a lethal dose of LPS (25 mg/kg). To our surprise, the survival study demonstrated significantly increased mortality in KO mice with Sag deficient myeloid cells (Figure 1B). We next measured LPS-induced proinflammatory cytokines production and observed that the levels of TNFα and IL-6 in the sera of KO mice were significantly higher than those of WT mice at 18 h after LPS injection (Figures 1C,D). These

surprising data suggested that mice with LysM Sag deficiency were hypersensitive to LPS.

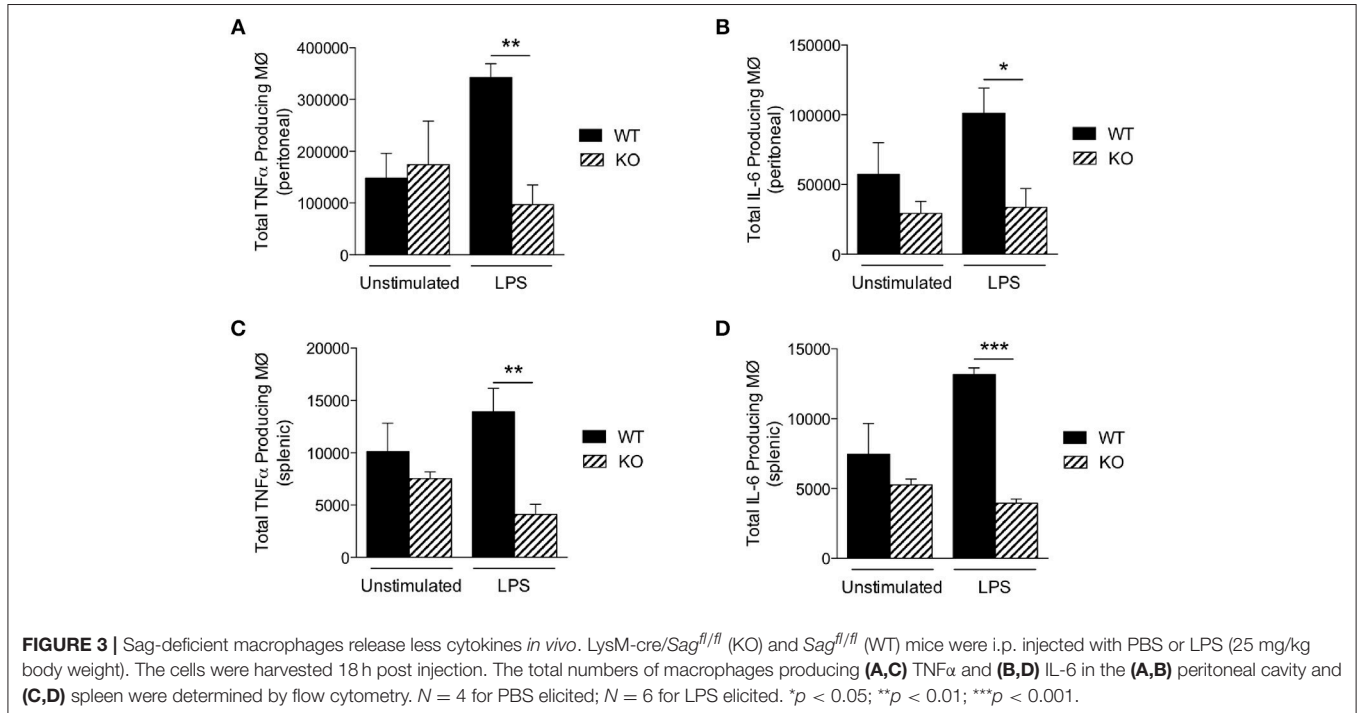
The *in vitro* Responses of Sag-Deficient Macrophages to LPS

Previous studies have demonstrated that SAG regulates other innate immune cell responses, such as DCs (16) and macrophages during infection (9). We next analyzed the response of Sag-deficient peritoneal macrophages stimulated with LPS. We observed that the release of the proinflammatory cytokines TNFα

TABLE 3 | Elicited macrophages.

Organ	Marker	WT (LyzM ⁻)	KO (LyzM ⁺)	P value
Peritoneal macrophages	PBS elicited	3.69e6 ± 4.88e5	4.71e6 ± 9.13e5	0.43
	LPS elicited	2.19e6 ± 9.11e5	2.19e6 ± 2.55e5	0.99
Splenic macrophages	PBS elicited	8.04e7 ± 1.80e7	7.14e7 ± 2.60e6	0.66
	LPS elicited	9.30e7 ± 1.24e7	8.73e7 ± 1.31e7	0.82

Shown are mean ± SD. *n* = 4 for PBS elicited, *n* = 6 for LPS elicited.



and IL-6 were significantly reduced by Sag-deficient macrophages (Figures 2A,B) with a similar decrease in mRNA transcripts for TNF α and IL-6 (Figures 2C,D) from these cells.

Studies have shown that inactivation of SAG reduces the viability of tumor cells and infected murine macrophages *in vitro* (9, 27). However, primary bone marrow derived DCs did not exhibit increased apoptosis upon inhibition of SAG E3 ligase complex (16) suggesting that inactivation of SAG in healthy, non-cancerous cells may not affect cell survival. Thus, we next tested whether primary WT and Sag-deficient macrophages stimulated with LPS resulted in altered cell viability. Once again, we observed no difference between WT and Sag-deficient peritoneal macrophages (Figure 2E).

To ensure that the results observed were not specific to macrophages isolated from a particular compartment, we next examined bone marrow derived macrophages (BMDMs). Consistent with our results from peritoneal macrophages, no significant differences in viability of BMDMs from WT or KO mice were observed (Figure 2F). Furthermore, LPS-induced release of TNF α and IL-6 cytokines by BMDMs over a total time period of 12 h, was significantly reduced

in the absence of Sag (Figures 2G,H). These data together suggest that Sag deficiency in macrophages significantly impairs the production of proinflammatory cytokines in response to LPS stimulation, but had no significant effect on the viability.

Sag Deficient Macrophages Release Less Cytokines *in vivo*

To further explore why KO mice were hypersensitive to LPS, we next measured LPS-induced production of proinflammatory cytokines *in vivo*. We injected LPS intraperitoneally (25 mg/kg) and then analyzed macrophages of the peritoneum and spleen by flow cytometry 18 h later. However, although the total numbers of macrophages were comparable between WT and KO mice (Table 3), the numbers of TNF α and IL-6 producing macrophages from the peritoneum (Figures 3A,B) and spleen (Figures 3C,D) were significantly lower in KO animals, compared to WT (Figure 3). Taken together, these data suggest that in the absence of Sag in myeloid cells, mice show (1) increased LPS-induced mortality, (2) increased proinflammatory cytokines in the sera, but (3) the increased mortality was not due to increased cytokine

release from the macrophages. Thus, these data indicated that the increase in proinflammatory cytokines contributing to mortality might be from another type of myeloid cell capable of responding to LPS and secreting increased proinflammatory cytokines.

Impact of Sag Deficiency in Macrophages: I κ B Accumulation

We next pursued the mechanism by which *Sag* deletion causes reduction of proinflammatory cytokines with focus on I κ B α /NF- κ B, since our previous studies have shown that I κ B α is a direct substrate of SAG E3 ligase (11). SAG disruption prevents the activation and translocation of NF- κ B, which contributes to decreased inflammatory cytokines from DCs and to the increased radiosensitivity observed in *Sag*-null murine embryonic stem cells (11, 16). Upon stimulation of a cell by TLR4, I κ B α is phosphorylated and degraded as a direct substrate of SAG-SCF $^{\beta-TrCP}$ E3 ubiquitin ligase (11). To determine if I κ B α and NF- κ B play a similar role in macrophages as was previously shown in dendritic cells (16), we examined the protein levels of phosphorylated and total I κ B in macrophages and found that LPS stimulation resulted in accumulation of phosphorylated I κ B α as well as total I κ B α in *Sag*-deficient macrophages (Figure 4A), indicating that the degradation of I κ B was impaired in the absence of *Sag*. Consistent with this notion, we found that the translocation of p65 NF- κ B from the cytoplasm to the nucleus was reduced in *Sag*-deficient macrophages compared to *Sag*-competent WT controls, as shown in Figure 4B, in which Parp and Procaspase-3 serve as biomarkers of nuclear and cytoplasmic fractions, respectively. These data suggest that similar to the effects seen in DCs, *Sag* disruption affects LPS-induced I κ B α degradation, which inhibits NF- κ B activation in macrophages, leading to reduced levels of proinflammatory cytokines, such as TNF α and IL-6.

Sag Deficiency Increases Proinflammatory Responses by Neutrophils

Similar to macrophages, neutrophils are myeloid lineage cells, which also express *LysM*. Thus, to determine the origin of increased LPS-induced cytokine production in the sera of mice with *Sag* deficient myeloid lineage cells, we next analyzed the response of neutrophils (CD11b $^+$ and Gr-1 $^+$) to LPS stimulation. We stimulated whole splenocyte cultures with LPS for 6 h (Figure 5A) and 18 h (Figure 5B) and observed a significant increase of TNF α expression in *Sag*-deficient CD11b $^+$ Gr-1 $^+$ -neutrophils (Figures 5A,B).

As NF- κ B is the transcription factor for TNF α , we next examined the translocation of NF- κ B from the cytoplasm to the nucleus in neutrophils. In contrast to the results seen in macrophages (Figure 4B), we did not find a difference in the translocation of NF- κ B in neutrophils (Figure 5C). These data suggested that *Sag* had a differential role in neutrophils, as compared with macrophages.

Previous studies have shown that LPS stimulation activates several intracellular signaling pathways including NF- κ B pathways in macrophages (28). To explore why *Sag* deficiency

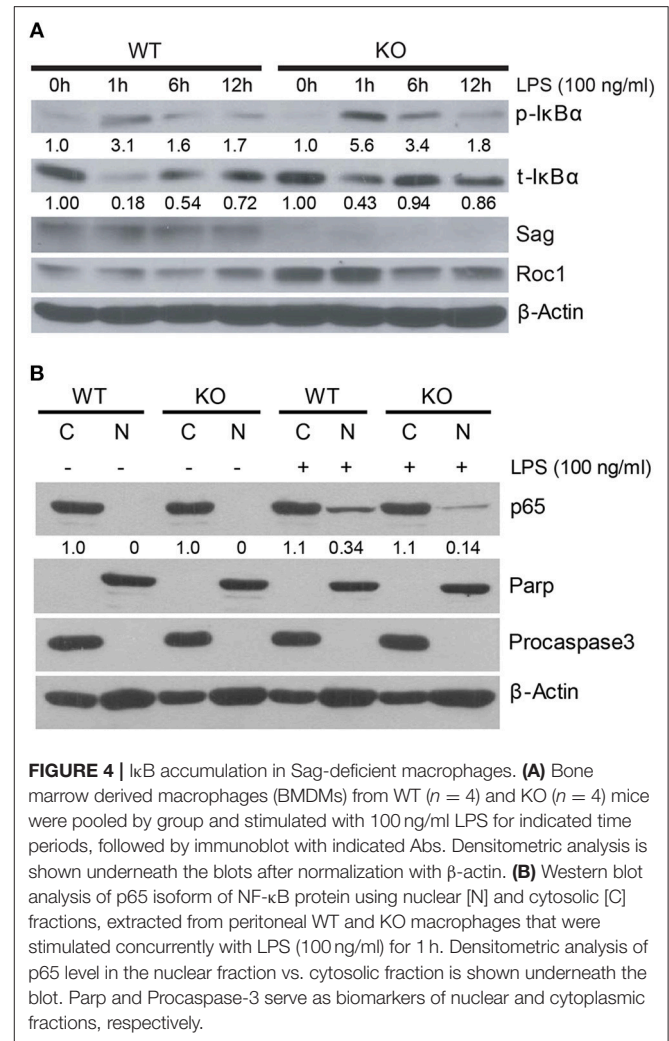


FIGURE 4 | I κ B accumulation in *Sag*-deficient macrophages. **(A)** Bone marrow derived macrophages (BMDMs) from WT ($n = 4$) and KO ($n = 4$) mice were pooled by group and stimulated with 100 ng/ml LPS for indicated time periods, followed by immunoblot with indicated Abs. Densitometric analysis is shown underneath the blots after normalization with β -actin. **(B)** Western blot analysis of p65 isoform of NF- κ B protein using nuclear [N] and cytosolic [C] fractions, extracted from peritoneal WT and KO macrophages that were stimulated concurrently with LPS (100 ng/ml) for 1 h. Densitometric analysis of p65 level in the nuclear fraction vs. cytosolic fraction is shown underneath the blot. Parp and Procaspase-3 serve as biomarkers of nuclear and cytoplasmic fractions, respectively.

in neutrophils causes an increase in TNF α release in contrast to what was observed in macrophages, we analyzed the mRNA transcripts in bone marrow cells from *LysM-Cre $^-$ /Sag $^{fl/fl}$* (WT) and *LysM-Cre $^+$ /Sag $^{fl/fl}$* (KO) mice in response to LPS. *Sag* deficiency was first confirmed in the bone marrow from KO mice by RT-PCR analysis (Supplemental Figure 3A). Microarray analysis revealed that the expression of 1,141 genes was specifically altered in response to LPS in *Sag*-deficient bone marrow cells (Figure 5D). Gene ontology (GO) analysis was then performed to enrich several sets of genes associated with multiple processes and pathways (Supplemental Figure 3B), including a list of genes responsive to LPS (Figure 5E, Supplemental Figure 3C). More importantly, we validated the microarray results by qRT-PCR and found that the induction of *Mpo*, the major enzyme to mediate the protective function of neutrophils from LPS-induced toxicity (17), and *Elane*, Neutrophil expressed elastase, was remarkably decreased in bone marrow cells from KO mice after LPS stimulation (Figure 5F). Furthermore, qRT-PCR results also confirmed that the expression of *LitaF* (LPS-induced TNF α factor), an important mediator of LPS-induced inflammatory response (29),

Cullin-5, the substrate of SAG-mediated neddylation and a scaffold component of SAG-CRL5 E3 ubiquitin ligase complex, also reduced proinflammatory cytokine production in sera and improved mice survival in response to LPS stimulation by repressing TRAF6 polyubiquitination to impair TRAF6-dependent NF- κ B activation (34). Consistently, our *in vivo* study demonstrated that the deficiency of Sag suppressed the production of proinflammatory cytokines in macrophages (Figures 2, 3). By contrast, we observed significantly increased TNF α production in Sag-deficient CD11b⁺ Gr-1⁺-neutrophils (Figures 5A,B) and a net increase of proinflammatory cytokine production in the sera from LysM-Cre⁺/Sag^{fl/fl} mice after LPS stimulation (Figures 1C,D). The reasons for the differential response to Sag deficiency in macrophages and neutrophils are unclear at the present time. We propose that these responses are likely due to differences in cell context in which different Sag substrates are targeted for degradation in a cell-type specific manner. Indeed, the degradation of I κ B α is inhibited in macrophages (Figure 4A) and dendritic cells (16), leading to the inhibition of NF- κ B nuclear translocation, which is not seen in neutrophils upon Sag deletion (Figure 5C). It is worth noting that MLN4924 was recently shown to inhibit the production of proinflammatory cytokines in response to LPS in purified peritoneal neutrophils (35). However, MLN4924 pretreatment followed by LPS stimulation for 4 h had no significant effects on the viability of neutrophils in that study.

Innate immune signaling is poorly understood. Our finding that Sag protein plays a differential role in macrophages and neutrophils is significant and novel as it is the first demonstration that Sag function can be determined by targeting—or not targeting—I κ B α in two types of critical cells of the innate immune system. This observation is consistent with our recent finding that Sag plays a tissue specific role during Kras-triggered tumorigenesis, in which Sag functions as a Kras-cooperator in the lung (19), or Kras-antagonist in the skin (36). Our microarray analysis on bone marrow provided some mechanistic insights (Figures 5D,E). Specifically, deletion of Sag in bone marrow cells causes decreased induction of Mpo and Elane, two cytoprotective proteins specifically expressed in neutrophils in response to LPS (Figure 5F). Mpo, a major peroxidase expressed mainly in neutrophils to produce cytotoxic and microbicidal reactive oxidants during inflammatory response (37, 38), plays a protective role during LPS-induced endotoxemia (17). Moreover, Mpo-deficient mice exhibited elevated levels of blood cytokines and chemokines, and increased mortality in response to LPS (17). Consistent with this study, we found that the induction of Mpo in response to LPS was decreased in Sag-deficient bone marrow cells (Figure 5F). It is known that neutrophils are the major source of Mpo after LPS challenge *in vivo* (17). Thus, our

finding suggests that the decreased induction of Mpo from KO mice might be associated with the increased levels of TNF α and IL-6 in sera and significantly greater susceptibility of KO mice to LPS (Figures 1B–D). In addition, the decreased induction of Elane, also known as neutrophils elastase, which is a serine protease expressed by neutrophils to degrade bacteria during inflammation (18), was found in Sag-deficient bone marrow in response to LPS. This may reduce host defense against invading pathogens, leading to the increased LPS-induced mortality in KO mice with Sag deficient myeloid cells. Future studies will be directed to further dissect the underlying mechanism by which Sag positively regulates the expression of Mpo and Elane in neutrophils.

In summary, our findings demonstrate that Sag protein differentially regulates inflammatory responses of myeloid cell subsets. In macrophages, disruption of Sag reduces the release of inflammatory cytokines by preventing the degradation of I κ B α , which blocks translocation of NF- κ B to the nucleus. In neutrophils, disruption of Sag has no effects on nuclear translocation of NF- κ B, but may impair the induction of Mpo and Elane in response to LPS stimulation, which increases the release of inflammatory cytokines and thus likely contributing to the increased mortality *in vivo* in response to LPS.

AUTHOR CONTRIBUTIONS

XX and NM designed and performed the experiments, analyzed and interpreted the data, and drafted the manuscript. HuL, MT, and HF performed the experiments. HaL analyzed the data. PR and YS designed the work, analyzed and interpreted the data, and revised the manuscript. All authors reviewed the manuscript.

ACKNOWLEDGMENTS

This work is supported by National Key R&D Program of China (2016YFA0501800) to YS and XX; by National Cancer Institute grants (R01 CA156744 and CA171277) to YS; and by National Institutes of Health grants (National Heart, Lung and Blood Institute, HL-090775 and HL-128046; and National Cancer Institute, CA-173878) to PR. NM was supported by a Post-doctoral Fellowship, PF-17-042-01–LIB, from the American Cancer Society.

SUPPLEMENTARY MATERIAL

The Supplementary Material for this article can be found online at: <https://www.frontiersin.org/articles/10.3389/fimmu.2018.02882/full#supplementary-material>

REFERENCES

- Akira S, Uematsu S, Takeuchi O. Pathogen recognition and innate immunity. *Cell* (2006) 124:783–801. doi: 10.1016/j.cell.2006.02.015
- Silva MT. When two is better than one: macrophages and neutrophils work in concert in innate immunity as complementary and cooperative partners of a myeloid phagocyte system. *J Leukoc Biol.* (2010) 87:93–106. doi: 10.1189/jlb.0809549
- Razani B, Reichardt AD, Cheng G. Non-canonical NF-kappaB signaling activation and regulation: principles and perspectives. *Immunol Rev.* (2011) 244:44–54. doi: 10.1111/j.1600-065X.2011.01059.x

4. Takeuchi O, Akira S. Pattern recognition receptors and inflammation. *Cell* (2010) 140:805–20. doi: 10.1016/j.cell.2010.01.022
5. Spooner R, Yilmaz O. The role of reactive-oxygen-species in microbial persistence and inflammation. *Int J Mol Sci.* (2011) 12:334–52. doi: 10.3390/ijms12010334
6. Swaroop M, Bian J, Aviram M, Duan H, Bisgaier CL, Loo JA, et al. Expression, purification, and biochemical characterization of SAG, a ring finger redox-sensitive protein. *Free Radic Biol Med.* (1999) 27:193–202. doi: 10.1016/S0891-5849(99)00078-7
7. Duan H, Wang Y, Aviram M, Swaroop M, Loo JA, Bian J, et al. SAG, a novel zinc RING finger protein that protects cells from apoptosis induced by redox agents. *Mol Cell Biol.* (1999) 19:3145–55. doi: 10.1128/MCB.19.4.3145
8. Sun Y, Li H. Functional characterization of SAG/RBX2/ROC2/RNF7, an antioxidant protein and an E3 ubiquitin ligase. *Protein Cell* (2013) 4:103–16. doi: 10.1007/s13238-012-2105-7
9. Chang SC, Ding JL. Ubiquitination by SAG regulates macrophage survival/death and immune response during infection. *Cell Death Differ.* (2014) 21:1388–98. doi: 10.1038/cdd.2014.54
10. Chang FM, Reyna SM, Granados JC, Wei SJ, Innis-Whitehouse W, Maffi SK, et al. Inhibition of neddylation represses lipopolysaccharide-induced proinflammatory cytokine production in macrophage cells. *J Biol Chem.* (2012) 287:35756–67. doi: 10.1074/jbc.M112.397703
11. Tan M, Zhu Y, Kovacev J, Zhao Y, Pan ZQ, Spitz DR, et al. Disruption of Sag/Rbx2/Roc2 induces radiosensitization by increasing ROS levels and blocking NF-kappaB activation in mouse embryonic stem cells. *Free Radic Biol Med.* (2010) 49:976–83. doi: 10.1016/j.freeradbiomed.2010.05.030
12. Zhou L, Zhang W, Sun Y, Jia L. Protein neddylation and its alterations in human cancers for targeted therapy. *Cell Signal.* (2018) 44:92–102. doi: 10.1016/j.cellsig.2018.01.009
13. Li L, Liu B, Dong T, Lee HW, Yu J, Zheng Y, et al. Neddylation pathway regulates the proliferation and survival of macrophages. *Biochem Biophys Res Commun.* (2013) 432:494–8. doi: 10.1016/j.bbrc.2013.02.028
14. Lawrence T. The nuclear factor NF-kappaB pathway in inflammation. *Cold Spring Harb Perspect Biol.* (2009) 1:a001651. doi: 10.1101/cshperspect.a001651
15. Tak PP, Firestein GS. NF-kappaB: a key role in inflammatory diseases. *J Clin Invest.* (2001) 107:7–11. doi: 10.1172/JCI11830
16. Mathewson N, Toubai T, Kapeles S, Sun Y, Oravec-Wilson K, Tamaki H, et al. Neddylation plays an important role in the regulation of murine and human dendritic cell function. *Blood* (2013) 122:2062–73. doi: 10.1182/blood-2013-02-486373
17. Reber LL, Gillis CM, Starkl P, Jönsson F, Sibilano R, Marichal T, et al. Neutrophil myeloperoxidase diminishes the toxic effects and mortality induced by lipopolysaccharide. *J Exp Med.* (2017) 214:1249–58. doi: 10.1084/jem.20161238
18. Kessenbrock K, Frohlich L, Sixt M, Lammermann T, Pfister H, Bateman A, et al. Proteinase 3 and neutrophil elastase enhance inflammation in mice by inactivating antiinflammatory progranulin. *J Clin Invest.* (2008) 118:2438–47. doi: 10.1172/JCI34694
19. Li H, Tan M, Jia L, Wei D, Zhao Y, Chen G, et al. Inactivation of SAG/RBX2 E3 ubiquitin ligase suppresses KrasG12D-driven lung tumorigenesis. *J Clin Invest.* (2014) 124:835–46. doi: 10.1172/JCI70297
20. Tan M, Li H, Sun Y. Endothelial deletion of Sag/Rbx2/Roc2 E3 ubiquitin ligase causes embryonic lethality and blocks tumor angiogenesis. *Oncogene* (2014) 33:5211–20. doi: 10.1038/onc.2013.473
21. Weischenfeldt J, Porse B. Bone Marrow-Derived Macrophages (BMM): isolation and applications. *CSH Protoc.* (2008) 2008:prot5080. doi: 10.1101/pdb.prot5080
22. Tan M, Zhao Y, Kim SJ, Liu M, Jia L, Saunders TL, et al. SAG/RBX2/ROC2 E3 ubiquitin ligase is essential for vascular and neural development by targeting NF1 for degradation. *Dev Cell* (2011) 21:1062–76. doi: 10.1016/j.devcel.2011.09.014
23. Tan M, Davis SW, Saunders TL, Zhu Y, Sun Y. RBX1/ROC1 disruption results in early embryonic lethality due to proliferation failure, partially rescued by simultaneous loss of p27. *Proc Natl Acad Sci USA.* (2009) 106:6203–8. doi: 10.1073/pnas.0812425106
24. Irizarry RA, Hobbs B, Collin F, Beazer-Barclay YD, Antonellis KJ, Scherf U, et al. Exploration, normalization, and summaries of high density oligonucleotide array probe level data. *Biostatistics* (2003) 4:249–64. doi: 10.1093/biostatistics/4.2.249
25. Kamburov A, Pentchev K, Galicka H, Wierling C, Lehrach H, Herwig R. ConsensusPathDB: toward a more complete picture of cell biology. *Nucleic Acids Res.* (2011) 39:D712–7. doi: 10.1093/nar/gkq1156
26. Clausen BE, Burkhardt C, Reith W, Renkawitz R, Forster I. Conditional gene targeting in macrophages and granulocytes using LysMcre mice. *Transgenic Res.* (1999) 8:265–77. doi: 10.1023/A:1008942828960
27. Jia L, Yang J, Hao X, Zheng M, He H, Xiong X, et al. Validation of SAG/RBX2/ROC2 E3 ubiquitin ligase as an anticancer and radiosensitizing target. *Clin Cancer Res.* (2010) 16:814–24. doi: 10.1158/1078-0432.CCR-09-1592
28. Guha M, Mackman N. LPS induction of gene expression in human monocytes. *Cell Signal.* (2001) 13:85–94. doi: 10.1016/S0898-6568(00)00149-2
29. Tang X, Metzger D, Leeman S, Amar S. LPS-induced TNF-alpha factor (LITAF)-deficient mice express reduced LPS-induced cytokine: evidence for LITAF-dependent LPS signaling pathways. *Proc Natl Acad Sci USA.* (2006) 103:13777–82. doi: 10.1073/pnas.0605988103
30. Mathewson ND, Fujiwara H, Wu SR, Toubai T, Oravec-Wilson K, Sun Y, et al. SAG/Rbx2-dependent neddylation regulates T-cell responses. *Am J Pathol.* (2016) 186:2679–91. doi: 10.1016/j.ajpath.2016.06.014
31. Chang SC, Choo WQ, Toh HC, Ding JL. SAG-UPS attenuates proapoptotic SARM and Noxa to confer survival advantage to early hepatocellular carcinoma. *Cell Death Discov.* (2015) 1:15032. doi: 10.1038/cddiscovery.2015.32
32. Chang SC, Ding JL. SAG-UPS regulates malignant transformation—from chronic inflammation to pro-tumorigenesis to liver cancer. *Cell Death Dis.* (2015) 6:e1941. doi: 10.1038/cddis.2015.312
33. Soucy TA, Smith PG, Milhollen MA, Berger AJ, Gavin JM, Adhikari S, et al. An inhibitor of NEDD8-activating enzyme as a new approach to treat cancer. *Nature* (2009) 458:732–6. doi: 10.1038/nature07884
34. Zhu Z, Wang L, Hao R, Zhao B, Sun L, Ye RD. Cutting edge: a Cullin-5–TRAF6 interaction promotes TRAF6 Polyubiquitination and Lipopolysaccharide signaling. *J Immunol.* (2016) 197:21–6. doi: 10.4049/jimmunol.1600447
35. Jin J, Jing Z, Ye Z, Guo L, Hua L, Wang Q, et al. MLN4924 suppresses lipopolysaccharide-induced proinflammatory cytokine production in neutrophils in a dose-dependent manner. *Oncol Lett.* (2018) 15:8039–45. doi: 10.3892/ol.2018.8333
36. Xie CM, Wei D, Zhao L, Marchetto S, Mei L, Borg JP, et al. Erbin is a novel substrate of the Sag-betaTrCP E3 ligase that regulates KrasG12D-induced skin tumorigenesis. *J Cell Biol.* (2015) 209:721–37. doi: 10.1083/jcb.2014.11104
37. Nauseef WM. Myeloperoxidase in human neutrophil host defence. *Cell Microbiol.* (2014) 16:1146–55. doi: 10.1111/cmi.12312
38. Aratani Y. Myeloperoxidase: its role for host defense, inflammation, and neutrophil function. *Arch Biochem Biophys.* (2018) 640:47–52. doi: 10.1016/j.abb.2018.01.004

Conflict of Interest Statement: The authors declare that the research was conducted in the absence of any commercial or financial relationships that could be construed as a potential conflict of interest.

Copyright © 2018 Xiong, Mathewson, Li, Tan, Fujiwara, Li, Reddy and Sun. This is an open-access article distributed under the terms of the Creative Commons Attribution License (CC BY). The use, distribution or reproduction in other forums is permitted, provided the original author(s) and the copyright owner(s) are credited and that the original publication in this journal is cited, in accordance with accepted academic practice. No use, distribution or reproduction is permitted which does not comply with these terms.